Needleless electrospun phytochemicals encapsulated nanofibre based 3-ply biodegradable mask for combating COVID-19 pandemic

Nikhil Avinash Patil [a], Prakash Macchindra Gore [a,c], Niranjana Jaya Prakash [a], Premika Govindaraj [b], Ramdayal Yadav [c], Vivek Verma [d], Dhivya Shanmugarajan [e], Shivanand Patil [f], Abhay Kore [f], Balasubramanian Kandasubramanian [a,*]

[a] Nanofibre & Nano Surface Texturing Laboratory, Department of Metallurgical and Materials Engineering, Defence Institute of Advanced Technology, Ministry of Defence, Girinagar, Pune 411025, Maharashtra, India
[b] Materials Science and Engineering at the Factory of Future - Swinburne University of Technology, Hawthorn 3122, Victoria, Australia
[c] Institute for Frontier Materials, Deakin University, Waurn Ponds Campus, Geelong 3216, Victoria, Australia
[d] Synthesis and Solid State Pharmaceutical Centre, Department of Chemical Sciences, Bernal Institute, University of Limerick, V94T9PX Limerick, Ireland
[e] Department of Life Sciences, Altem Technologies, Platinum Partner of Dassault Systemes, Bangalore 560095, Karnataka, India
[f] Siddheshwar Techtessile Pvt. Ltd., Kolhapur 416012, Maharashtra, India

ARTICLE INFO

ABSTRACT

The emergence of COVID-19 pandemic has severely affected human health and world economies. According to WHO guidelines, continuous use of face mask is mandatory for personal protection for restricting the spread of bacteria and virus. Here, we report a 3-ply cotton-PLA-cotton layered biodegradable face-mask containing encapsulated phytochemicals in the inner-filtration layer. The nano-fibrous PLA filtration layer was fabricated using needleless electrospinning of PLA & phytochemical-based herbal-extracts. This 3-layred face mask exhibits enhanced air permeability with a differential pressure of 35.78 Pa/cm^2 and superior bacterial filtration efficiency of 97.9% compared to conventional face masks. Close-packed mesh structure of the nano-fibrous mat results in effective adsorption of particulate matter, aerosol particles, and bacterial targets deep inside the filtration layer. The outer hydrophobic layer of mask exhibited effective blood splash resistance up to a distance of 30 cm, ensuring its utilization for medical practices. Computational analysis of constituent phytochemicals using the LibDock algorithm predicted inhibitory activity of chemicals against the protein structured bacterial sites. The computational analysis projected superior performance of phytochemicals considering the presence of stearic acid, oleic acid, linoleic acid, and Arachidic acid exhibiting structural complementarity to inhibit targeted bacterial interface. Natural cotton fibers and PLA bio-polymer demonstrated promising biodegradable characteristics in the presence of in-house cow-dung based biodegradation slurry. Addition of jaggery to the slurry elevated the biodegradation performance, resulting in increment of change of weight from 07% to 12%. The improved performance was attributed to the increased sucrose content in biodegradation slurry, elevating the bacterial growth in the slurry. An innovative face mask has shown promising results for utilization in day-to-day life and medical frontline workers, considering the post-pandemic environmental impacts.

1. Introduction

Outbreak of the infectious SARS-CoV2 disease has drastically affected health of the global population, causing long time effects on respiratory systems of the human body [1]. According to the World Health Organization, spread of virus can be controlled using personal protective equipment such as face masks, protective suits, and face shields [2]. Global outbreak of the infectious virus has emerged with the need of an effective face mask for containing the spread of infectious aerosol particles, since most infectious respiratory disease causing viruses such as Influenza A are majorly transmitted through aerosol particles [3]. To restrain the spread of virus, conventionally available disposable non-woven surgical face mask and respirators were recommended for respiratory protection [4]. However, working principle of the mask was focused on physical blocking of pathogens in the air. Live infectious pathogens on the surface of mask are primary source for

contamination during the reuse or disposal of PPE [5]. Alternatively, the cloth mask is significantly advantageous for constraining the spread of virus due to better reusability and filtration of nano-scale aerosol particles in the air [6]. Among the conventional cloth masks, multiple layered face masks were recorded to showcase better results in restricting the spread of aerosol particles [7].

Incorporation of the electrospun nano-fibrous layer in multi-layered face mask structure has resulted in showcasing ameliorated filtration capabilities of the face mask [8,9]. Electrospun nano-fibrous mats have been crucial in capturing the tiny particulate matter with efficiencies of more than 99% [10]. The nano and micro structured membranes have showcased significant application in separation and purification technologies [11]. Fine fiber diameter of the electrospun nano-fiber facilitates increment in specific surface area of filter media, resulting in efficient filtration capabilities of the nano-fibrous layer [12,13]. Further, the micro structured surface morphology determines the filtration capabilities of the electrospun layer, whereas interfacial adhesion between the fibers facilitates formation of close-packed structure, which help in improving the filtration performance of the membranes [14,15]. Surface porosity and chemically functionalized surface of the nano-fibrous membranes has crucial impacts on filtration capabilities of nano-membranes, facilitating the ameliorated performance for capturing micro-sized particulate matter [16]. While maintaining the high filtration efficiency, low-pressure drop across the filter media carries vast importance in determining breathability of face mask [17]. Many commercialized fibers such as glass fibers, cellulose fibers, and melt-blown fibers have been investigated for their filtration performance, but the presence of micro-fiber diameter limits the further filtration performance of those fibers [18]. The utilization of single-use disposable non-woven face mask in filter media has resulted in the release of microplastics in the environment [19,20]. These microfibers released in the water reservoirs affects aquatic life and humankind by accumulating used face masks into landfills, resulting in deterioration of the ecological system [21,22], also, the release of microfibers in the human body may propagate invasive pathogens in the body [23]. On the contrary, utilization of the cloth material based face masks have been significantly crucial for exhibiting adequate filtration efficiency and reusability of the face mask for daily use [24,25]. Several bio-based materials are also reported to exhibit enhanced air filtration capacities, providing a balance between filtration capabilities and antimicrobial activity [26].

In addition to the ameliorated performance of electrospun nano-fibrous layer, addition of immune-boosting chemicals has a significant role in controlling the effects of infectious viruses and bacteria [27–29]. The injection mode for immune-boosting drugs and vaccines is effective through inhalation, reducing the efforts of trained medical staff's and becoming significantly advantageous in resource-poor regions. Predominantly, herbal plants or spices' extracts have potent effects against the activity of dreadful airborne viruses [30–32]. Xingjiang Xiong et al. have reported the biological activity of Chinese herbal extracts-based medicine, capable of combating the SARS-CoV-2 virus [33]. Glucocorticoids based drug treatment for SARS-CoV-2 have shown promising results by reducing the mechanical ventilation and mortality rate among COVID-19 patients compared to standard care protocol. Glucocorticoids were evident intervention for reducing the mechanical ventilation (31 fewer per 1000 patients, 47 fewer to 9 fewer, moderate certainty) and death rate (risk difference 37 fewer per 1000 patients, 95% credible interval 63 fewer to 11 fewer, moderate certainty) when compared with standard care [34]. Iveta Bartonkova et al. have demonstrated the activity of essential oils on glucocorticoid receptor; biological activities of essential oils were analyzed to have anti-microbial, anti-inflammatory, anti-hypertensive, and anti-fungal properties, enhancing the immunity of the human body against dreadful viruses [35]. The quantitative structure–toxicity relationship (QSTR) analysis of plant-derived herbal oils are recorded to be non-toxic, biodegradable, no irritancy at a lower concentration, and non-mutagenic.

Wide usage of non-woven face mask for restraining the spread of

COVID-19 pandemic has led to serious environmental impacts; resulting in increment of drastic effects on living ecological systems [36]. These environmental impacts encourage the research to develop an environment-friendly and biodegradable mask for combating infectious diseases [37]. The biodegradable fibers such as polylactic acid based electrospun nano-fiber layer have exhibited promising results for effective filtration of air and aerosol particles in the environment [38]. The nature-derived polymeric material has showcased microbial and enzymatic biodegradation studies as recorded in various investigations [39–44]. The other cellulosic component of the 3-ply face mask has demonstrated excellent biodegradation characteristics of the material [45]. The biodegradation slurry consisting of compost culture has shown encouraging results for degradation of cotton fabrics [46]. The immune-boosting herbal extracts present in the nano-fibrous PLA filtration layer have been reported to exhibit adequate biodegradability without affecting the environmental system [47].

The current study is focused on the fabrication of cotton/PLA based biodegradable mask showcasing the antiviral, anti-bacterial, and breathable characteristics. The major experiments of the investigation are focused on – (1) Fabrication of 3-layered mask, whose upper and lower fabric being consisting of cotton, and the middle layer comprising of an electrospun nano-fibrous Poly (lactic acid) layer functionalized with traditional Indian herbal extracts. (2) Utilization of traditional herbal extracts, demonstrated effective performance in neutralizing the effect of bacteria and viruses [48–51]. (3) Computational analysis of phytochemicals using the advanced scoring function based LibDock Algorithm, showcasing the ameliorated performance of herbal-extracts in neutralizing the bacteria. Furthermore, it demonstrated immune-boosting characteristics under controlled dosage through inhalation. (4) Characterization of the filter media of 3-ply mask to evaluate bacterial filtration efficiency, air permeability, and blood splash resistance, for determining the product's effectiveness among medical frontline workers and citizens for day-to-day use. The analysis of a mask's surface wettability has a crucial role in the reusability of a mask after multiple piles of washing. (5) Biodegradation characteristics of face masks are evaluated for analyzing the after effects of used face mask, in order to minimize the environmental impacts due to pandemic.

2. Materials and methods

Poly-(lactic acid) (PLA) (FIBREEL, white colour, 1.75 mm diameter) was procured from Rever Industries, Nashik, India. Dichloromethane (99% pure) was procured from Thermo Fisher Scientific India Pvt Ltd, which is utilized as a solvent for dissolving the PLA polymer. 100% cotton fabric material (thickness of 0.33 mm, 150 GSM, warp and weft count of 20 × 20 respectively, ends and picks per inch of 56 × 56) was procured from the local fabric market. Azadirachta Indica has been extracted from Agri based neem seeds, procured from local farmers in Pune, India. The herbal extracts of Eucalyptus Citriodora were procured from Vishal Chemicals, Mumbai, India. A digital thickness meter gauge was used to evaluate the film thickness of the 3-ply biodegradable mask's layered structure. C6-Fluorocarbon based dispersion solution named TUBIGUARD 30-F, and the cross-linking agent TUBICOAT FIX H26 (used for improving the washing durability of the fabric) was procured from CHT Group Germany. The binary solution mixture of TUBIGUARD 30-F and TUBICOAT FIX H26 was spray-coated on the Cotton fabric using a hand-operated spray gun with a distance of 20 cm from the nozzle tip.

2.1. Needleless electrospinning of PLA nano-fibrous membrane

The polymer solution was prepared by dissolving 15 wt% of premium quality PLA polymer beads in dichloromethane (DCM) solvent. Dissolution of the PLA polymer was carried out at room temperature in the presence of continuous magnetic stirring at 200 rpm speed. Traditional Indian herbal extracts of *Azadirachta Indica* (10 wt% with respect

to PLA) and *Eucalyptus Citriodora* (10 wt% with respect to PLA) were added to the polymer solution and mixed thoroughly to achieve a homogeneous solution. Viscosity of polymer solution was analyzed using a Brookfield Viscometer to determine the spinning characteristics of polymer solution. The polymer solution was then subjected to needleless electrospinning using the pilot scale plant machine i.e. Model: Nanospider[TM] Make: Elmarco s.r.o., Czech Republic, at Ahmedabad Textile Industry's Research Association (ATIRA) (as per assembly in Fig. 1). In the needleless electrospinning assembly, the distance between two electrodes was fixed at 18 cm for obtaining a nano-fibrous layer. Voltage at the collector electrode was adjusted to −30 kV, whereas the rotating electrode voltage was maintained at 60 kV for facilitating the effective formation of nano-fibers. The rotating electrode speed was fixed at 6 rpm for deposition of a nano-fibrous layer on base cotton fabric at the collector terminal. Cotton fabric at the collector electrode was processed at a speed of 0.5 m/min, 1 m/min, 2 m/min, and 3 m/min for depositing the nano-fibrous layer. An optimum closely packed nano-fibrous layer was achieved at the collector electrode speed of 1 m/min. The optimization of collector processing time was carried out by measuring thickness of nano-fiber layer on base cotton fabric using a digital thickness meter gauge.

2.2. Scanning electron microscopy and atomic force microscopy

Surface morphology of the PLA nano-fibrous layer on base of cotton fabric was analyzed using the Field Emission Scanning Electron Microscopy (FE-SEM, Carl-Zeiss AG, JSM-6700F, Germany). Morphology of the nano-fibrous layer was recorded for evaluating the compactness in surface area of the electrospun PLA nano-fibers on the cotton surface. Furthermore, morphology of the biodegraded samples was recorded to analyze the change in morphology of face mask after subjecting to the thorough biodegradation process.

Further morphological analysis of the nanofibers was evaluated using atomic force microscopy (Model : Asylum Research MFP3D, Make: Oxford Instruments, UK) at room temperature ($25 \pm 3\,°C$), with a scanning area of 05 μm, and total area of $127\,μm^2$. AFM analysis helps in understanding the surface roughness patterns, symmetrical variations of the surface, sand porosity of the surface in a quantified form.

2.3. Air permeability assessment

The air breathability assessment of face mask was carried out using IS 16289:2014 Annex C standard to measure the differential pressure [52]. IS 16289:2014 measures air resistance using a flow meter (as per Fig. 2). The standard technique can be used to measure an airflow of 8 L/min. The mask's testing sample should provide five different circular test areas of 2.5 cm orifice diameter (cumulative area of $4.9\,cm^2$). This standard assessment determines the breathability of mask material by evaluating the pressure difference in air flow through filter media of mask material. As reported in the standard operating procedure, the air is passed through an inlet valve, and a flowmeter is connected at the inlet of assembly displays the flow rate of air into the assembly, and further, the air is passed through the testing sample for evaluating the change in pressure using two manometers. The pressure difference in air among the inlet and outlet of filter media determines the breathability of mask [52]. The differential pressure drop across filter media is mathematically expressed as per equation (1).

$$\Delta P = \frac{X_{m1} - X_{m2}}{Area\ of\ test\ material\ (cm^2)} \tag{1}$$

X_{m1} = mean water pressure in manometer 1 (mm of water) of the five test areas, across the low pressure side of material.

X_{m2} = mean water pressure in manometer 2 (mm of water) of five test areas, across the high pressure side of material.

2.4. Bacterial filtration efficiency

Bacterial filtration efficiency (BFE) of the face mask was evaluated using the IS 16,288 standard technique [53]. The standard procedure determines the efficiency by passage of bacteria containing aerosol through the filtering layer of face mask. According to the standard technique, analysis was carried out using Staphylococcus Aureus ATCC 6538 test bacteria with an inoculum size of 5×10^5 CFU/mL in presence of tryptic soya agar media. The peptone water was used as a dilution media, and testing is carried out at incubation conditions of $37 \pm 2\,°C$ for 24 h. The BFE testing on a face mask was facilitated by the face-sided test sample having an area of 10×10 cm, and the sample was conditioned at a temperature of $21 \pm 5\,°C$. The flow rate of bacteria-containing aerosols was adjusted to 28.5 L/min, exhibiting mean particle size of the challenging aerosols fixed to 3.0 ± 0.3 μm. The bacterial aerosols were delivered to the test sample using a peristaltic pump in presence of controlled air pressure. The flow rate of the aerosol particles passing through the cascade impactor was adjusted to 28.3 L/min, where the duration of bacterial aerosol delivery time was fixed to 2 min. The agar
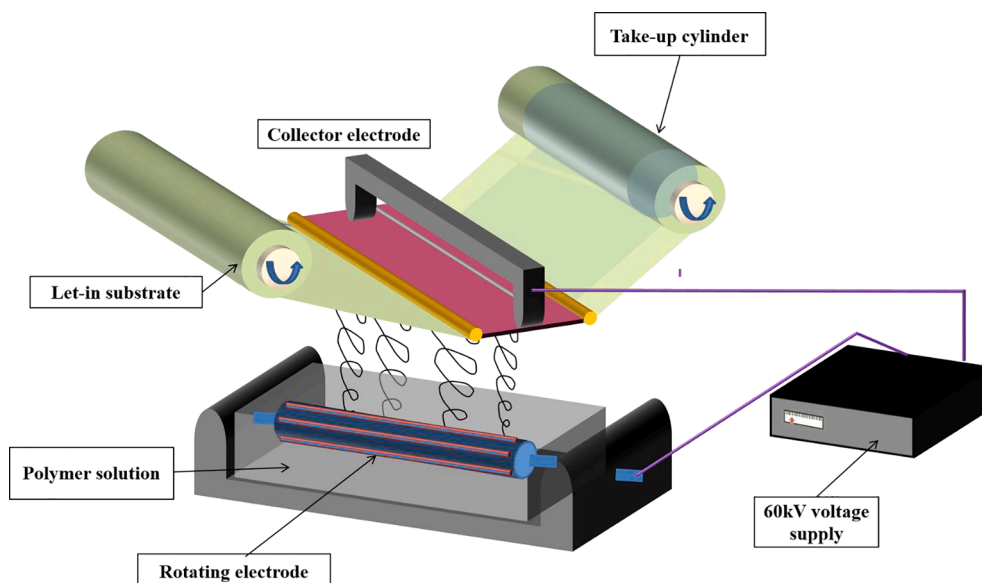

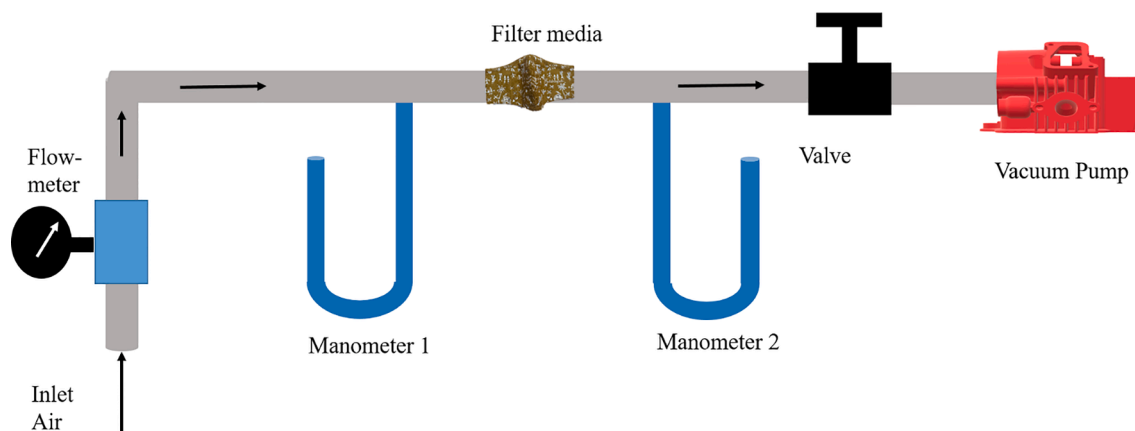**Fig. 1.** Assembly for needleless electrospinning of polymer solution.

Fig. 2. Working principle for testing of air permeability by using standard IS 16289:2014.

plates were placed into the cascade impactor, and testing samples are clamped on top of it. After the passage of bacterial aerosol for 2 min, the samples were evaluated for BFE [53]. The mathematical expression for calculating BFE is as per equation (2).

$$Bacterial\ filtration\ efficiency\ \% = \frac{(C - T) \times 100}{C} \qquad (2)$$

C: Average plate count total for test control
T: Plate count total for testing sample

2.5. Splash resistance test

Splash resistance of the 3 ply face mask using the synthetic blood was evaluated using IS 16289:2014 Annex D standards [52]. According to the standard procedure, mask samples were conditioned at temperature conditions of $27 \pm 2\ °C$ and $65 \pm 2\%$ relative humidity for replicating the moisture equilibrium at standard environmental conditions. The testing sample was mounted on sample holding fixture such that the inside surface of face mask should be completely visible. The mask sample testing was carried out by dispensing a controlled volume of synthetic blood (approximately 2 ml) through a small diameter cannula (internal diameter of 0.084 cm, and 1.27 cm long) over the conditioned mask sample, under the pressure of 120 mm of Hg. The mask's testing sample was placed at a distance of 30.5 cm for achieving adequate replication of blood splash. Inner side of face mask was observed through the viewing hole (within 10 sec) in presence of suitable lighting to evaluate the penetration of synthetic blood [52].

2.6. Surface wetting test (Contact angle measurement)

The surface wetting characteristics of 3-ply mask were evaluated using a contact angle goniometer (model no. DSA 25E, Kruss GmbH, Germany). Measurement of the wetting contact angle (WCA) was facilitated using a standardized 8 μL droplet of deionized water (DI) at room temperature. WCA was recorded on the cotton-PLA-cotton interface and PLA-cotton interface, by placing a drop of DI water on the surface interface. The standard contact angle was measured using a Young-Laplace fitting method in the software. Each sample was repeated for minimum 4 times and then the final average of values was taken as a standard contact angle. These investigations were crucial to understand the hydrophilic and hydrophobic characteristics of the mask, which helps in understanding the washability for reuse and the specific performance of the components in 3-ply mask.

2.7. Computational study of the phytochemicals

Computational analysis of the herbal phytochemicals against the potential target bacterial proteins was performed using the docking score functioned LibDock Algorithm [54,55]. LibDock is a high-throughput algorithm for docking ligands into an active receptor site, aligning ligand conformations to polar and apolar receptor interaction hotspots, and reports the best scoring poses. The ligand conformations with receptor sites profoundly depend on the structural properties, rotation of bonds, and binding energy [56]. The interaction's docking characteristics were optimized using the Broyden Fletcher Goldfarb Shanno algorithm and consistent force field minimization. Heat map analysis is superior to the dot map or picto-trendline to analyze the spread of infectious disease [57].

The retrieval of proteins and ligands at the 5 drug target site is sourced from the PDB structural database. The theoretical models of the protein and ligand structures were validated and utilized to analyze the docking score. Major phytochemical constituents of the medicinal *Azadirachta indica* and *Eucalyptus citriodora* herbal oils were obtained from the PubChem compound database. The raw protein structures sourced from the protein data bank (PDB) database were further prepared for docking studies by removing all the hetatms and explicit HOH atoms. The docking studies were performed to understand the effective binding performance of the phytochemicals by removing destructive steric clashes, and alternative conformations, insert missing atoms in incomplete residues, and modeling missing loop regions, and standardizing the atom names. The interactions between receptor and ligand were investigated by analyzing molecular docking, using structural molecular biology and CADD. The purpose of this stochastic protein–ligand interaction analysis is hypothesized to probe an enhanced performance of phytochemicals and their mechanism for inhibiting protein structures of the targeted site by utilizing ligands structures.

2.8. Biodegradation

Biodegradation studies of the 3-ply mask were evaluated using a cow dung based slurry [58]. The biodegradation slurry was prepared by adding 50 g of fresh cow dung (derived from local farm) into one-liter water, and the mixture was stirred to achieve proper mixing of components in the biodegradation slurry. The initial weight of mask samples was recorded, and samples were immersed in the biodegradation slurry for 30 days. After 30 days, test samples were removed from the slurry and subjected to washing using water. Washed samples were dried in oven at $70\ °C$ for 2 h, to remove the moisture content from biodegraded samples. Final weight of test samples was measured to evaluate the reduction in weight of the face mask after biodegradation. Jaggery was used to enhance the growth of microorganisms in the biodegradation process; hence 50 g jaggery was added to the biodegradation slurry. Fresh samples of the face mask were weighed and added into the biodegradation slurry for 20 days. The samples were removed from biodegradation slurry and washed thoroughly. The washed samples

were dried in the oven at 70 °C for a duration of 2 h, followed by an evaluation of the final weight. Effectiveness of the biodegradation process was assessed depending upon the change in weight (%) of the face mask samples using following equation (3).

$$\text{Weight change }(\%) = \frac{(\textit{Final weight of sample after biodegradation} - \textit{Initial weight of sample}) \times 100}{\textit{Initial weight of sample}} \tag{3}$$

3. Results and discussions

3.1. Fabrication and characterization of needleless electrospun layer

Bacterial filtration efficiency and air permeability of the face mask are highly dependent upon the nano-fibrous electrospun PLA filter media due to its compact structure and enhanced surface area for adsorption on the nano-fibrous layer [59]. Multiple studies have been focused on development of PLA nano-fibrous mats using the conventional electrospinning system (single nozzle electrospinning technique) [60,61]; however, the low productivity rate of this process is restricting the industrialization of conventional process [62,63]. Hence, the current study has been focused on the needleless electrospinning technique of the nano-fibers on base cotton surface, considering the industrial viability of the designed product in pandemic times. Needleless electrospun nano-fibrous layers are substantially crucial for the formation of highly porous, small pore sized, and internally connected porous structured PLA electrospun mats [38]. Industrially scalable needleless electrospinning technique is highly beneficial for developing uniform electrospun mats, with an average fiber diameter of 8 ± 0.2 μm (calculated using ImageJ software). Fiber diameter is sensitive towards the viscosity of electrospinning solution, distance between the electrodes, and strength of electrostatic field; whereas the thickness of electrospun mats is affected by the duration of fiber deposition and speed of rotation of the collecting electrode [64]. At the optimum collector electrode speed of 1 m/min, mean thickness of the needleless electrospun nano-fibrous layer is recorded to be 0.41 mm (calculated using digital thickness meter gauge). As per our previous investigation [40], the viscosity of herbal extracts containing PLA polymer solution at a rate of 10 rpm was found to be 950 cP at ambient temperature conditions (27 °C). The fine fiber diameter of PLA electrospun mats results in ameliorated surface area for aerosol particles' adsorption on the surface [65]. PLA nano-fibrous layer removes the large particle size of aerosols and particulate

matter from the substrate's surface, whereas the fine particles are captured deeper inside the close-packed electrospun filter media [66]. The needleless electrospinning technique has emerged as a novel technique for developing industrially scalable nano-fibrous mats for applications in advanced air filter media [67–69]. Nano-fibers have characteristic properties of improved surface adhesion, low basis weight with uniform fiber diameter, high porosity, and specific surface area, leading to its utilization as an excellent air filter media [70,71]. As per the FE-SEM in Fig. 3 (A), uniformity in fiber diameter and dense nano-fibers structure in the needleless electrospun mats, leads to the steady and stable filtration stage in the purification of particulate matter and bacteria from the air The fine diameter nano-scaled highly porous structured electrospun mats [as per Fig. 3 (B)] plays a crucial role in the filtration of air, by adsorbing the particulate material and volatile organic gases [11,16]. According to the Frazier analysis, the needleless electrospun PLA nano-fibrous layer has mean pore size of 20.1429 μm, maximum pore size distribution of 5.0400, and mean flow pore pressure of 0.604 psi. The stable air filtration is caused due to adsorption of the impurities according to 5 specific mechanisms – (i) Interception, (ii) Brownian diffusion, (iii) Gravity effect, (iv) Electrostatic effect, and (v) Inertial impaction [72]. These mechanisms may show variations in the nano-fibrous layer's filtration efficiencies, whereas total filtration efficiency is calculated by the cumulative aggregate of all these mechanisms considering the size and shape of impurities in air [73]. Compact and multi-layered structure of face masks is crucial to demonstrate the enhanced results for filtration of micro aerosol particles. Increment in layers of face mask has been proven to increase filtration efficiency and differential pressure of the face mask, enhancing the protection from harmful pathogens and viruses [74]. In the present study, 3-ply Cotton-PLA-Cotton mask recorded face mask's breathability due to low differential pressure of 35.78 Pa/cm^2. The mask recorded bacterial filtration efficiency of 97.9%, with an average plate count of positive control of *Staphylococcus aureus* ATCC 6538 bacteria as 2168 (as per supporting data, Fig. S1). The face mask has received CE certification from United Kingdom Approval System for Certification Bodies Limited (Certificate No.: 17020) based on the optimum performance of face mask (as per supporting data, Fig. S2).
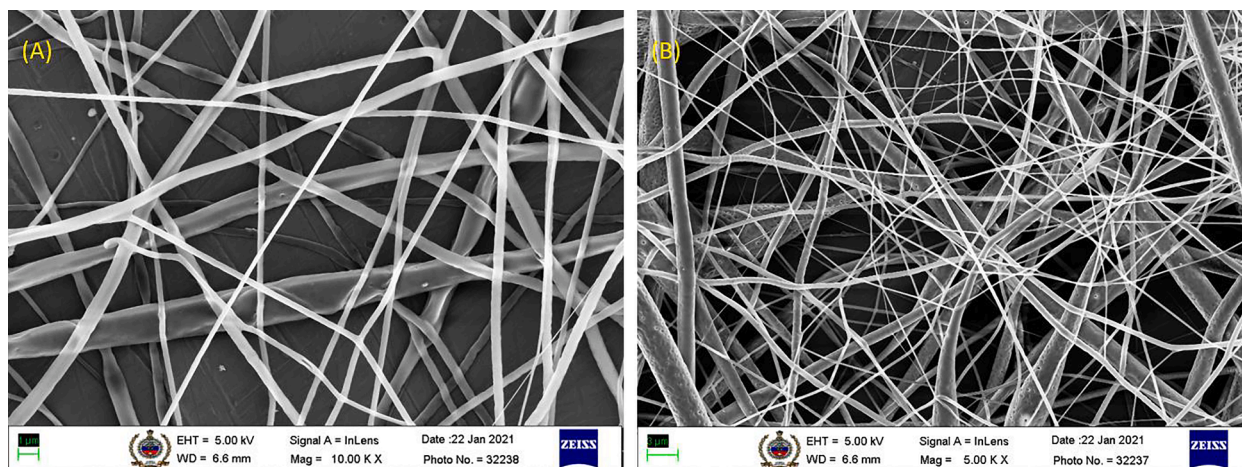

Fig. 3. FE-SEM micrographs of PLA nano-fibrous layer at (A) magnification of 1 μm, and accelerating voltage of 5 kV, (B) magnification of 3 μm, and accelerating voltage of 5 kV.
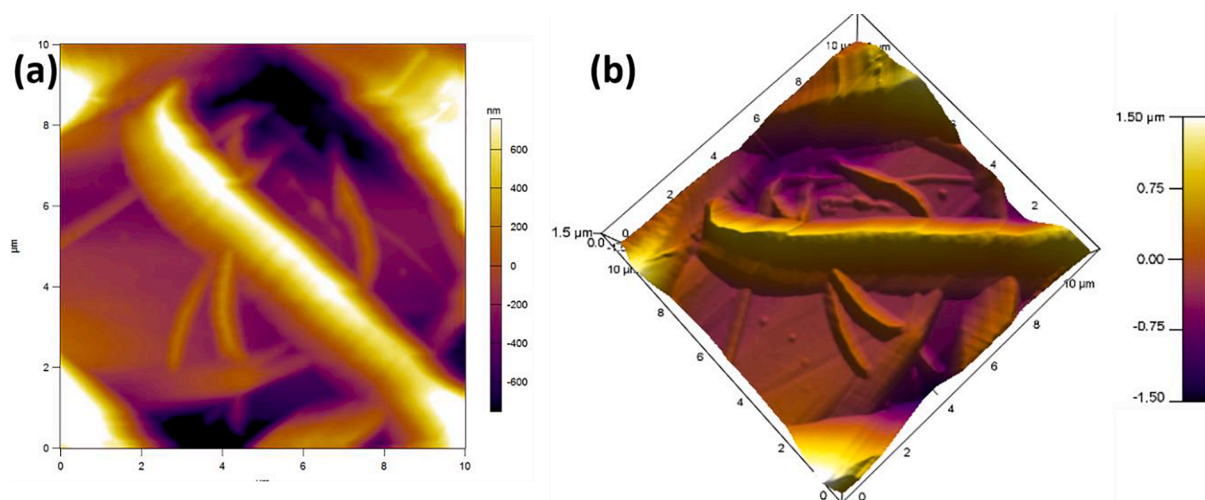
Fig. 4. AFM micrographs of developed PLA nanofibers revealing (a) 2D, and (b) 3D surface morphology.

Furthermore, the morphological analysis of the nanofibers was evaluated using atomic force microscopy (Model : Asylum Research MFP3D, Make: Oxford Instruments, UK) as shown in Fig. 4.

AFM analysis of developed PLA nanofibers performed on an rea of $127 \, \mu m^2$, showed a hierarchical surface morphology, with varying surface roughness which demonstrated a root mean square roughness value of $423 \pm 50 \, nm$ [27]. The symmetrical variations of surface were calculated using the roughness skewness value which is found to be 0.417. The distribution of nanofiber roughness around the mean surface was calculated using kurtosis value, which was found to be 0.328. The

surface roughness of the nanofibers directly influences its adhesion with the fabric surface (in this case, cotton fabric), and helps in maintaining the hydrophobic nature [40,75–77].

3.2. Surface wetting analysis

The wetting behavior of C6-fluorocarbon spray-coated cotton (Top Layer), Pristine cotton fabric (inner layer), PLA/Neem (middle layer) electrospun non-woven fabric towards water was analyzed using static contact angle method via contact angle goniometer. A C6-Fluorocarbon
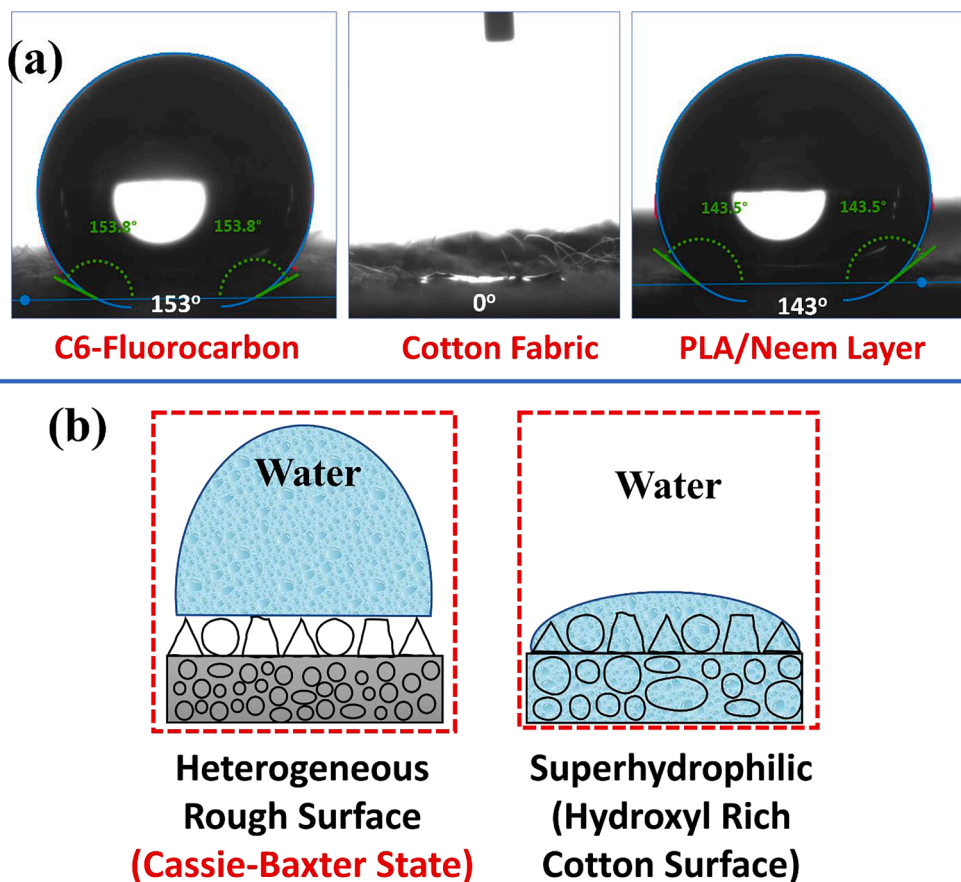

Fig. 5. (a) Contact angle measurements of the C6 fluorocarbon coated surface, cotton fabric surface, and PLA/Neem electrospun layer, (b) Cassie-Baxter state of the surface and superhydrophilic nature of the cotton fabric.

based dispersed solution (TUBIGUARD 30-F) rich in fluoro molecules is spray-coated [78] onto cotton fabric in such a way that it does not block the pores of the cotton microfibers and forms a thin layer of thickness of 0.05 mm. A molecule of C6 fluorocarbon contains 6 carbon atoms in the main molecular structure, which are bonded to various fluorine atoms, which react with the molecules of fabric surface during solution coating. Gavrilenko & Wang, De Smet et al., Rezíc and Kiš, and CHT Group Germany have reported the finishing of textiles using C6-Fluorocarbon for reducing the surface tension of coated surface, thereby improving water repellent property of the fabric [78–81].

The static water contact angles of C6-Fluorocarbon spray-coated cotton (Top Layer), Pristine Cotton fabric (inner layer), PLA/Neem (middle layer) electrospun non-woven fabric was found to be 153° (superhydrophobic nature), 0° (superhydrophilic) & 143° (hydrophobic nature), respectively [Fig. 5 (a)]. Pristine Cotton fabric was instantly saturated by water, i.e. superhydrophilic nature, principally influenced by the presence of abundantly available intrinsic hydroxyl groups like –OH, –CH$_2$OH, -H, and O˙ in its main cellulosic structure [40]. These hydroxyl groups possess affinity towards –OH⁻, and H⁺ molecular ions, thereby imparting water-absorbing nature, i.e. superhydrophilic, to cotton fabric [40] [Fig. 5 (a) & (b)]. Robert Zyschka from CHT Group

Germany, has further reported the action of C6 fluorocarbon, which assist in minimization of virus or bacteria-contaminated aerosols adsorption onto the outermost layer of the face mask, thereby reducing the risk of infection [78].

Hydrophobicity of the PLA-Neem electrospun layer is attributed to molecular groups like CH3, -C = O, and –CO, which possess polarity, i.e. charged state repels the ions present in water [40]. Further, the electrospinning action gives non-woven nature to the PLA/Neem fibers, which result in a surface exhibiting rough, porous, and heterogeneous morphology .

The collective action of charged molecular groups present in PLA and the porous heterogeneous rough surface of PLA/neem fibers help to render them hydrophobic nature [82]. The C6 fluorocarbon-based solution spray-coated on cotton fabric makes the surface highly rich with fluorine based-groups. The fluoro groups present on the fabric surface exhibit a high charge state, i.e. high electronegativity, due to the presence of fluorine atoms (-F⁻), and bonds firmly with cellulosic groups present on the cotton fabric. The highly polarized state and firm bonding of fluoro groups with the cotton fabric helps to render the superhydrophobic nature to the outer layer [79–81,83].

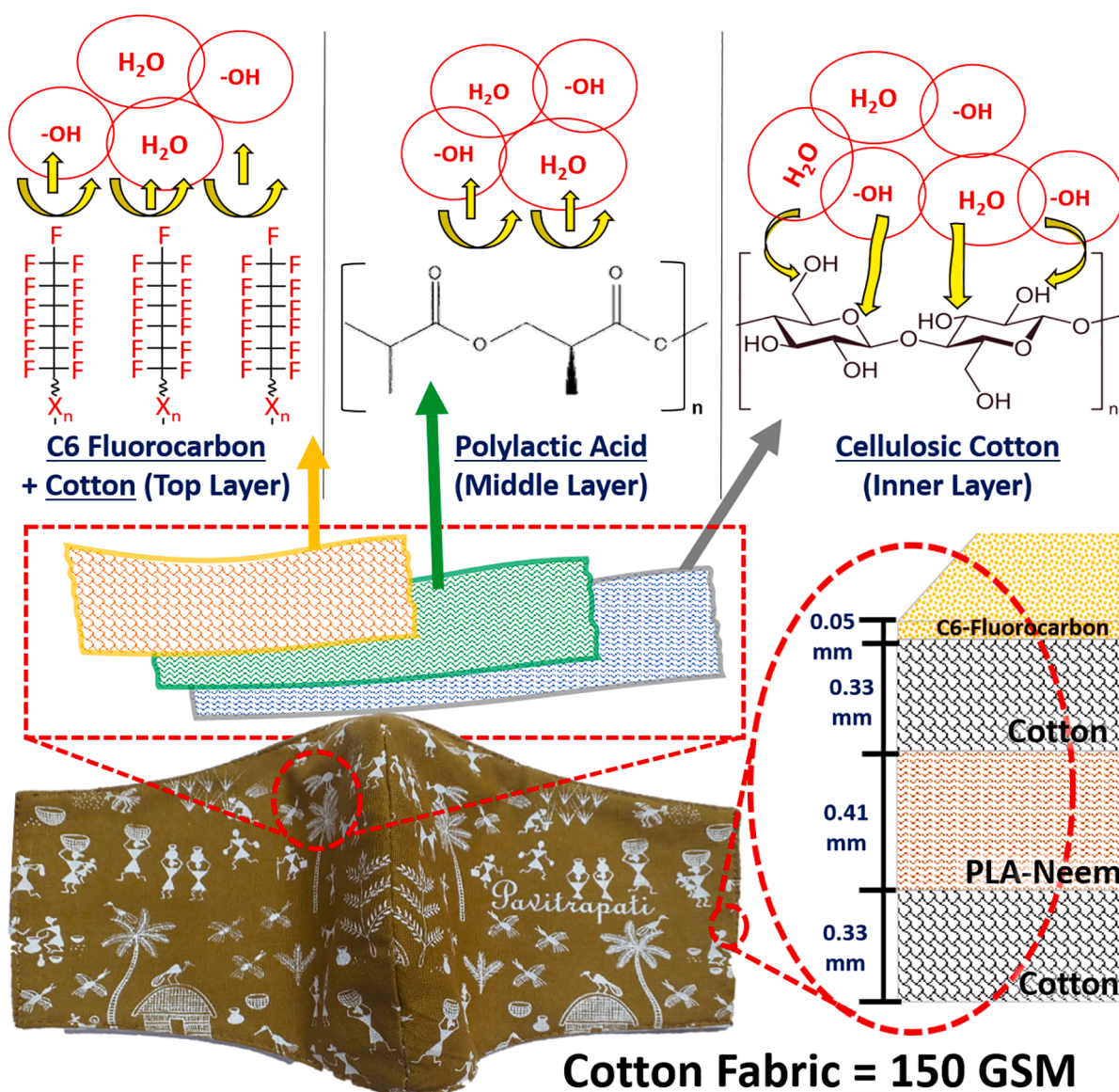The possible mechanism for interaction of water molecules with C6-

Fig. 6. Pictorial representation of water molecules' interaction with the top layer, middle layer, and the inner layers of the face mask.

Fluorocarbon spray-coated Cotton (Top Layer), Pristine Cotton fabric (inner layer), PLA/Neem (middle layer) electrospun non-woven is shown pictorially in Fig. 6.

The top layer of cotton and middle layer PLA of the face mask reveal porous, rough, heterogeneous textured surface morphology. The hydrophobic/superhydrophobic nature of any surface with porous and heterogeneous morphology is explained using Cassie-Baxter theory [Fig. 5 (b)]. Cassie-Baxter's theory is explained using the following equation [40,83,84].

$$cos\ \theta_c = f_1 cos\theta_1 - f_2 \qquad (4)$$

Where, θ_c = apparent contact angle,
$f_1 f_1$ & f_2 = surface-fractions of phase-1 and phase-2, respectively,
θ_1 = contact angle of phase-1.

Porous and rough morphology of the surface results in generation of air-pockets entrapped between pore and rough-textured surfaces, which act as air-pockets between pores and heterogeneous rough surfaces. These air-pockets hold entrapped air that repels water molecules and thereby restricts its entry inside the porous surface and the acting capillary forces. Gore et al. have stated that the small size of the pores existing on the surface exhibit a high capillary force of attraction considering the big-sized pores. Thus, the small-sized pores demand immense pressure to open up (in the present study, pressure needed for water to cross through the surface exhibiting superhydrophobic nature) [40,83–86].

3.3. Incorporation of encapsulated phytochemicals and their computational analysis

The increased demand for an anti-microbial filtration layer has motivated the researchers to incorporate the encapsulated nanoparticles, enhancing the bacterial inhibition of airborne microbes. An investigation by Jeongan Choi demonstrated the encapsulation of bio-based *Sophora flavescens* herbal extract nanoparticles enhances anti-microbial air filtration, with 99.99% filtration efficiency and 99.98% bacterial efficiency [87]. Nano-dispersed herbal extracts of *Azadirachta Indica* in the bi-layered electrospun mats were also reported to demonstrate anti-microbial characteristics for filtering the micro-scale particulate matter as well as bacteria [88]. The antibacterial activity of Azadirachta Indica and silver nanoparticles on electrospun polylactide fibers are demonstrated to exhibit improved bacterial filtration nano-membranes [89]. In addition to that, the presence of herbal extracts of *Eucalyptus Citriodora* has showcased antiviral characteristics against the infectious herpes simplex virus [90]. An investigation by Mariana Dias Antunes et al. has reported the anti-microbial activity of *Eucalyptus Citriodora* containing electrospun ultrafine fibers against gram-positive and gram-negative bacteria [91]. The utilization of encapsulated phytochemicals has resulted in its distinguishable characteristics of exhibiting antibacterial properties, restraining the spread of bacteria and viruses during the COVID-19 pandemic.

Computational analysis of the phytochemicals against proteins-structured bacteria and virus targets has been crucial for predicting the activity of constituent chemicals to inhibit the protein structure [92] (as per Fig. 7). Computational analysis of chemical constituents of traditional Indian herbal phytochemicals is carried out using scoring function based LibDock algorithm. *In silico* study analyzes the specific binding sites of protein–ligand complex and structural characteristics of the chemical phytochemicals against the multiple bacteria targets. Docking performance analyzes the structural complementarity of chemical constituents to investigate the neutralizing capabilities of herbal extracts against the bacterial targets. The selection of bacterial targets is based on its activity to restrain the spread of infectious COVID-
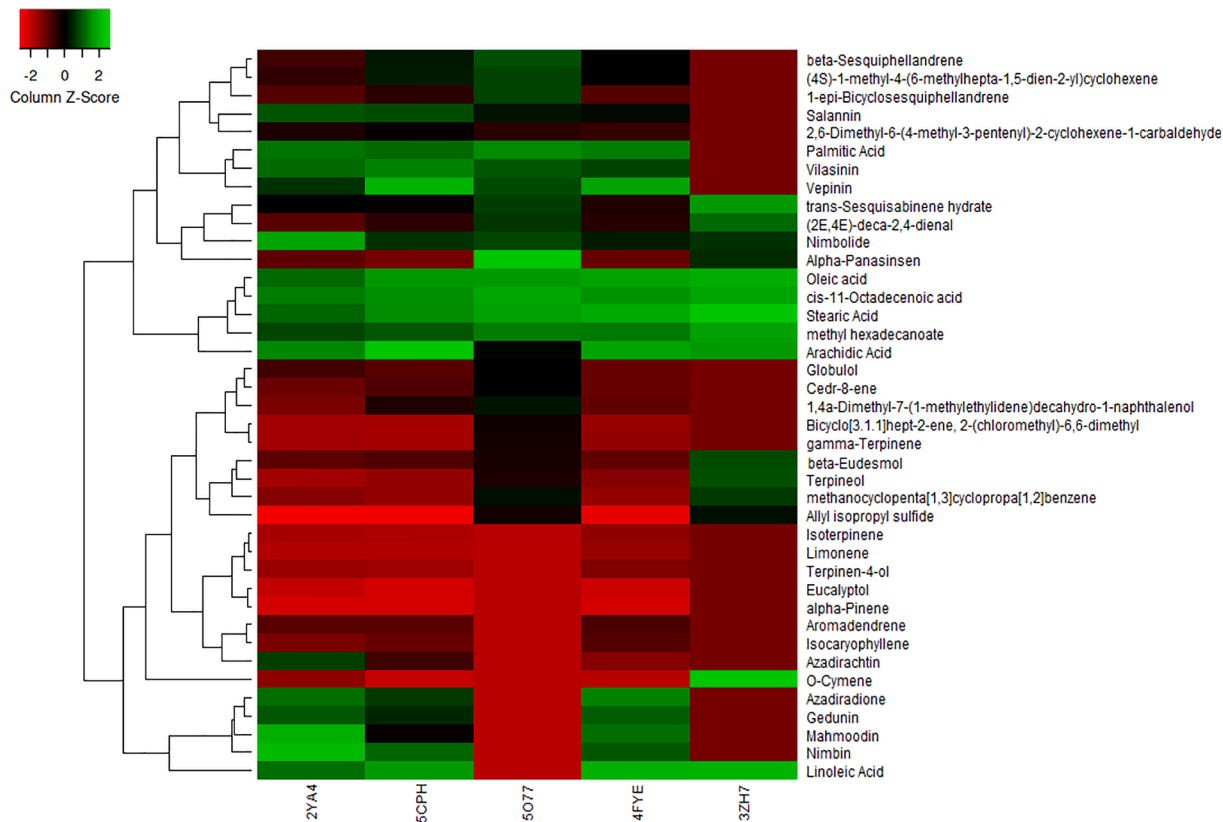

Fig. 7. Computational heat map analysis of herbal phytochemicals' chemical constituents containing *Azadirachta Indica* and *Eucalyptus Citriodora* against protein structures of the bacteria. *(2YA4- Neuraminidase (NA) protein from Streptococcus pneumonia, 5CPH- DNA gyrase subunit B from Staphylococcus aureus, 5O77 - OmpK35 from Klebsiella pneumonia, 4FYE- SidF form Legionella pneumophila, 3ZH7 - Protein E from Haemophilus Influenzae).*

19 virus. The neutralizing characteristics of the chemical constituents are attributed to their superior docking performance, and ability to undergo an interaction for unfolding of the protein structure. The superior docking score of Nimbin and Mahmoodin against the *2YA4- Neuraminidase (NA) protein from Streptococcus pneumonia* bacteria is due to the presence of hydrogen bond acceptor; it enhances the hydrogen bonding between the protein–ligand complex due to the attraction between acceptor's positive charge and electron lone pair on the other atom [93]. The neutralizing capabilities of Arachidic acid, Linoleic acid, oleic acid, and stearic acid against the protein structure of *5CPH- DNA gyrase subunit B from Staphylococcus aureus* is facilitated due to presence of aliphatic chains in their chemical structure. Presence of an aliphatic structure results in effective rotation of bonds to occupy the binding site, enhancing the docking score of phytochemical against the targeted protein site [94]. 3-ply mask containing the herbal extracts of traditional Indian herbs has exhibited a filtration efficiency of 97.9% against the same bacteria. Similarly, the inhibiting activity of alpha-panasinsen and *cis*-11-octadecanoic acid against the *5O77 - OmpK35 from Klebsiella pneumonia* is attributed to its aliphatic characteristics of the constituent phytochemicals, resulting in effective binding at the protein interface. Similarly, the structure complementarity of Arachidic acid and Stearic acid against *4FYE- SidF form Legionella pneumophila* have showcased an effective docking performance facilitating the ameliorated binding of ligands across the binding sites of protein structures due to presence of aliphatic bonds in their chemical structures. The inhibiting activity of stearic acid and o-cymene has been crucial for structural complementarity against the *3ZH7 - Protein E from Haemophilus Influenzae* bacteria. The computational studies has supported the antibacterial claims of traditional herbal phytochemicals against the protein structures of bacteria, assisting in restricting the spread of COVID-19 virus.

3.4. Biodegradation performance

Biodegradation of face masks is advantageous for combatting the post-pandemic environmental impacts of COVID-19 pandemic on the ecological systems. The release of synthetic microfibers from commercial non-woven masks into the environment may result in harmful effects on humankind. The present study has investigated the biodegradation characteristics of used face masks, immersing it into the biodegradation slurry consisting majorly of fresh cow-dung. The freshly prepared cow-dung slurry is used to investigate the biodegradation characteristics since the presence of bacteria in the cow-dung has been recorded to exhibit degradation of commodity plastics [58]. Cow-dung microflora consists of about 60 various types of bacteria, dominated by *Corynebacterium* sp., *Bacillus* sp., *Lactobacillus* sp., *Aspergillus*, and *trichoderma*. In addition to these, the cow-dung slurries contain about 100 species of protozoa and 2 yeasts [95]. The slurries have been reported to contain a various group of bacteria such as Serratia, Acinetobacter, and Alcaligenes spp [96,97], as plant growth-promoting bacteria. In the presence of composting conditions, naturally occurring polylactide films have showcased aerobic biodegradation characteristics [98], primarily undergoing hydrolytic cleavage of ester bonds in an aqueous medium to break the macromolecular chains [99]. In the present study, nano-fibrous PLA layer was completely degraded when immersed in the jaggery based biodegradation slurry. Degradation of PLA has been facilitated in the presence of organic waste to undergo anaerobic digestion [100]; similarly, the sugarcane bagasse has been

recorded to exhibit anaerobic biodegradation of cellulosic fibers [101,102]. Since the significant constituents of jaggery are sucrose, the additive accelerates the biodegradation rate of PLA and cotton fibers in the biodegradation slurry. The hydrophobic coating layer of C6-fluorocarbon is found to be biodegraded which is evident from the hydrophilic (water contact angle = 0°) nature of the top layer after biodegradation. The biodegrading microorganisms have most probably caused the scission of the bond between C6-fuorocarbon molecules and the cellulosic groups present in the cotton. Thus, the face mask showcased improved degradation as the change in the weight of mask sample increased from approx. 7% to approximately 12% (as per data of Tables 1 and 2).

Morphology of the PLA interface represented in Fig. 8 (A); demonstrates the growth of bacteria structures on the surface of biodegraded electrospun nano-fibrous layer. Whereas, the FE-SEM images in Fig. 8 (B) showcase the enhanced growth of bacteria on PLA nano-fiber surface. The enhanced bacterial growth colonies on the surface of PLA nano-fiber results in effective degradation of the face mask samples in presence of jaggery based biodegradation slurry. During the biodegradation process, minute organic particulate matter in the biodegradation slurry occupies the porous structures on the surface of PLA fiber, assisting in degradation of the PLA nanofibre layer. FE-SEM images in Fig. 8 (C) and (D) discloses the biodegraded cotton samples after subjecting to biodegradation slurry. The biodegradation process removes convolutions on the surface morphology of the cotton fibers, resulting in improved biodegradation characteristics of the face mask.

4. Conclusion

In the present study, we have reported the characteristics and performance of a 3-ply biodegradable face mask containing encapsulated phytochemicals to ameliorate bacterial filtration efficiency. The 3-ply layer mask consists of cotton-PLA-cotton interface; the inner nanofibrous PLA filtration layer is fabricated using electrospinning of the PLA dispersed in DCM solution. The encapsulated phytochemicals are incorporated in the electrospun filtration substrate by addition of phytochemicals in DCM solution (10 wt% of PLA). The three-layered face mask has demonstrated enhanced air permeability by showcasing the differential pressure of 35.78 Pa/cm^2, with a superior BFE of 97.9% compared to the other conventional masks available in the global markets. Ameliorated performance of 3-ply face mask is attributed to the electrospun nano-fibers, increasing the available surface area of the electrospun mats. The low fiber diameter of nano-fibers forms a close-packed mesh structure, resulting in adsorption of various particulate matter, aerosol particles, and bacterial targets deep inside the filtration layer. The 3-ply mask material has also exhibited blood splash resistance due to an outer hydrophobic layer of the face mask, ensuring its utilization for medical practices. Computational studies of the phytochemical nanoparticles using LibDock algorithm have exhibited improved inhibiting characteristics against the protein structured bacterial sites. Presence of stearic acid, oleic acid, linoleic acid, and Arachidic acid in phytochemicals have showcased promising results for unfolding of bacteria protein structures to inhibit the spread of bacteria. Cotton natural fibers and PLA bio-polymer have demonstrated promising biodegradable characteristics in the presence of the in-house developed cow-dung based biodegradation slurry. Addition of jaggery has increased the sucrose content in biodegradation slurry, elevating the

Table 1
Change in percent of weight of samples after immersing in biodegradation slurry of cow-dung and water for 30 days.

Sample	Initial weight (gm)	Final weight (gm)	Change in weight (%)
Sample 1	13.7422	12.8456	6.52%
Sample 2	14.3711	13.3867	6.85%
Sample 3	14.5671	13.5824	6.76%

Table 2
Change in weight (%) of samples after immersing in biodegradation slurry of cow-dung, Jaggery, and water for 20 days.

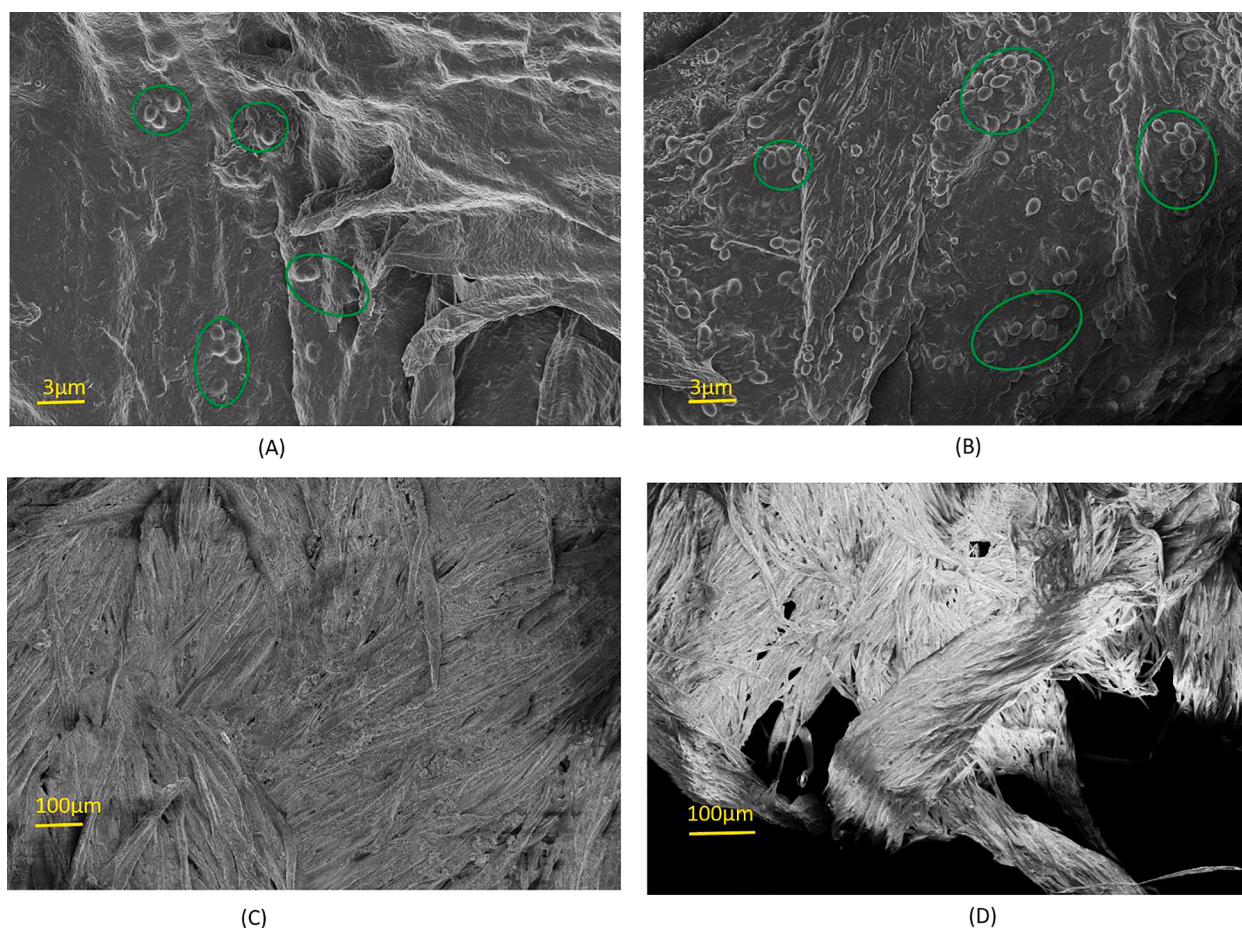| Sample	Initial weight (gm)	Final weight (gm)	Change in weight (%)
Sample 1	13.9521	12.2541	12.17%
Sample 2	14.5812	12.8417	11.93%
Sample 3	14.6596	12.8594	12.28%

Fig. 8. FE-SEM images of the biodegraded samples at accelerating voltage of 2.5 kV, (A) PLA surface after 30 days treatment in cow-dung and water containing biodegradation slurry, (B) PLA surface after 20 days treatment in cow-dung, jaggery and water containing biodegradation slurry, (C) Cotton surface after 30 days treatment in cow-dung and water containing biodegradation slurry, and (D) Cotton surface after 20 days treatment in cow-dung, jaggery and water containing biodegradation slurry.

bacterial growth and consequently improving the biodegradability of fibers in mask material. It has showcased 12% weight reduction after biodegradation for 20 days in cow-dung, jaggery, and water-based slurry. Hence, the development of the high bacterial efficiency 3-ply biodegradable face mask has exhibited promising results, considering the post-pandemic environmental impacts on the ecological systems.

Declaration of Competing Interest

The authors declare that they have no known competing financial interests or personal relationships that could have appeared to influence the work reported in this paper.

frontline workers, doctors, nurses, healthcare staff and workers, and all people who are contributing in combating the spread of COVID-19 pandemic. The authors are thankful to all anonymous Reviewers, and the Editor for providing the valuable comments, and suggestions, which helped in improving the quality of the revised manuscript.

Appendix A. Supplementary data

Supplementary data to this article can be found online at https://doi.org/10.1016/j.cej.2021.129152.

References

[1] E.A. Belongia, M.T. Osterholm, COVID-19 and flu, a perfect storm, Science (80-.) 368 (2020) 1163, https://doi.org/10.1126/science.abd2220.

[2] World Health Organization, Clinincal Management of COVID-19, 2020.

[3] S. Stelzer-Braid, B.G. Oliver, A.J. Blazey, E. Argent, T.P. Newsome, W. D. Rawlinson, E.R. Tovey, Exhalation of Respiratory Viruses by Breathing, Coughing, and Talking, J. Med. Virol. (2009), https://doi.org/10.1002/jmv.

[4] S. Bhattacharjee, P. Bahl, A.A. Chughtai, C.R. MacIntyre, Last-resort strategies during mask shortages: Optimal design features of cloth masks and decontamination of disposable masks during the COVID-19 pandemic, BMJ Open Respir. Res. 7 (2020) 1–10, https://doi.org/10.1136/bmjresp-2020-000698.

[5] L. Liao, W. Xiao, M. Zhao, X. Yu, H. Wang, Q. Wang, S. Chu, Y. Cui, Can N95 Respirators Be Reused after Disinfection? How Many Times? ACS Nano. 14 (2020) 6348–6356, https://doi.org/10.1021/acsnano.0c03597.

[6] C.R. MacIntyre, H. Seale, T.C. Dung, N.T. Hien, P.T. Nga, A.A. Chughtai, B. Rahman, D.E. Dwyer, Q. Wang, A cluster randomised trial of cloth masks compared with medical masks in healthcare workers, BMJ Open. 5 (2015), https://doi.org/10.1136/bmjopen-2014-006577.

[7] P. Bahl, S. Bhattacharjee, C. De Silva, A.A. Chughtai, C. Doolan, C.R. Macintyre, Face coverings and mask to minimise droplet dispersion and aerosolisation: A video case study, Thorax. (2020) 1–2, https://doi.org/10.1136/thoraxjnl-2020-215748.

[8] L. Mei, Y. Ren, Y. Gu, X. Li, C. Wang, Y. Du, R. Fan, X. Gao, H. Chen, A. Tong, L. Zhou, G. Guo, Strengthened and Thermally Resistant Poly(lactic acid)-Based Composite Nanofibers Prepared via Easy Stereocomplexation with Antibacterial Effects, ACS Appl. Mater. Interfaces. 10 (2018) 42992–43002, https://doi.org/10.1021/acsami.8b14841.

[9] V.V. Kadam, L. Wang, R. Padhye, Electrospun nanofibre materials to filter air pollutants – A review, J. Ind. Text. 47 (2018) 2253–2280, https://doi.org/10.1177/1528083716676812.

[10] I.M. Hutten, L. Wadsworth, Handbook of nonwoven filter media, 2007. 10.1016/B978-1-85617-441-1.X5015-X.

[11] J. Cui, T. Lu, F. Li, Y. Wang, J. Lei, W. Ma, Y. Zou, C. Huang, Flexible and transparent composite nanofibre membrane that was fabricated via a " green " electrospinning method for efficient particulate matter 2. 5 capture, J. Colloid Interface Sci. 582 (2021) 506–514, https://doi.org/10.1016/j.jcis.2020.08.075.

[12] A. Podgórski, A. Bałazy, L. Gradoń, Application of nanofibers to improve the filtration efficiency of the most penetrating aerosol particles in fibrous filters, Chem. Eng. Sci. 61 (2006) 6804–6815, https://doi.org/10.1016/j.ces.2006.07.022.

[13] B. Kandasubramanian, P. Govindaraj, Peeling model for cell adhesion on electrospun polymer nanofibres, J. Adhes. Sci. Technol. 28 (2014) 171–185, https://doi.org/10.1080/01694243.2013.833402.

[14] M. Zhang, J. Cui, T. Lu, G. Tang, S. Wu, W. Ma, C. Huang, Robust, functionalized reduced graphene-based nanofibrous membrane for contaminated water purification, Chem. Eng. J. 404 (2021), https://doi.org/10.1016/j.cej.2020.126347.

[15] H. Zhang, D. Hua, C. Huang, S.K. Samal, R. Xiong, F. Sauvage, K. Braeckmans, K. Remaut, S.C. De Smedt, Materials and Technologies to Combat Counterfeiting of Pharmaceuticals : Current and Future Problem Tackling, 1905486 (2020) 1–13. 10.1002/adma.201905486.

[16] J. Cui, F. Li, Y. Wang, Q. Zhang, W. Ma, C. Huang, Electrospun nano fi ber membranes for wastewater treatment applications, Sep. Purif. Technol. (2020), 117116, https://doi.org/10.1016/j.seppur.2020.117116.

[17] D. Cho, A. Naydich, M.W. Frey, Y.L. Joo, Further improvement of air filtration efficiency of cellulose filters coated with nanofibers via inclusion of electrostatically active nanoparticles, Polymer (Guildf). 54 (2013) 2364–2372, https://doi.org/10.1016/j.polymer.2013.02.034.

[18] Y. Li, X. Yin, J. Yu, B. Ding, Electrospun nanofibers for high-performance air filtration, Compos. Commun. 15 (2019) 6–19, https://doi.org/10.1016/j.coco.2019.06.003.

[19] T.A. Aragaw, Surgical face masks as a potential source for microplastic pollution in the COVID-19 scenario, Mar. Pollut. Bull. 159 (2020), 111517, https://doi.org/10.1016/j.marpolbul.2020.111517.

[20] O.O. Fadare, E.D. Okoffo, Covid-19 face masks: A potential source of microplastic fibers in the environment, Sci. Total Environ. 737 (2020), 140279, https://doi.org/10.1016/j.scitotenv.2020.140279.

[21] O.O. Fadare, B. Wan, L.H. Guo, L. Zhao, Microplastics from consumer plastic food containers: Are we consuming it? Chemosphere. 253 (2020) 126787 https://doi.org/10.1016/j.chemosphere.2020.126787.

[22] S. Rist, B. Carney Almroth, N.B. Hartmann, T.M. Karlsson, A critical perspective on early communications concerning human health aspects of microplastics, Sci. Total Environ. 626 (2018) 720–726, https://doi.org/10.1016/j.scitotenv.2018.01.092.

[23] A.J. Reid, A.K. Carlson, I.F. Creed, E.J. Eliason, P.A. Gell, P.T.J. Johnson, K. A. Kidd, T.J. MacCormack, J.D. Olden, S.J. Ormerod, J.P. Smol, W.W. Taylor, K. Tockner, J.C. Vermaire, D. Dudgeon, S.J. Cooke, Emerging threats and persistent conservation challenges for freshwater biodiversity, Biol. Rev. 94 (2019) 849–873, https://doi.org/10.1111/brv.12480.

[24] C.R.M. Abrar, A. Chughtai, H. Seale, Effectiveness of Cloth Masks for Protection Against Severe Acute Respiratory Syndrome Coronavirus 2, Emerg. Infect. Dis. 26 (2020) e1–e5.

[25] E. Mahase, Covid-19: What is the evidence for cloth masks? BMJ. 369 (2020), m1422 https://doi.org/10.1136/bmj.m1422.

[26] M. Zhu, R. Xiong, C. Huang, Bio-based and Photocrosslinked electrospun antibacterial nanofibrous membranes for air filtration, Carbohydr. Polym. (2018), https://doi.org/10.1016/j.carbpol.2018.09.075.

[27] M. Zhu, R. Xiong, C. Huang, Bio-based and photocrosslinked electrospun antibacterial nanofibrous membranes for air filtration, Carbohydr. Polym. 205 (2019) 55–62, https://doi.org/10.1016/j.carbpol.2018.09.075.

[28] R.S. Ambekar, B. Kandasubramanian, Antimicrobial Electrospun Materials, in: Inamuddin, R. Boddula, M.I. Ahamed, A.M. Asiri (Eds.), Electrospun Mater. Their Allied Appl., 1st ed., Scrivener Publishing LLC, Wiley, New York, 2020: pp. 483–514. 10.1002/9781119655039.ch17.

[29] S. Tandon, B. Kandasubramanian, S.M. Ibrahim, Silk-Based Composite Scaffolds for Tissue Engineering Applications, Ind. Eng. Chem. Res. 59 (2020) 17593–17611, https://doi.org/10.1021/acs.iecr.0c02195.

[30] S. Borkotoky, M. Banerjee, A computational prediction of SARS-CoV-2 structural protein inhibitors from Azadirachta indica (Neem), J. Biomol. Struct. Dyn. (2020) 1–11, https://doi.org/10.1080/07391102.2020.1774419.

[31] F. Benencia, M.C. Courrèges, Antiviral activity of sandalwood oil against Herpes simplex viruses-1 and -2, Phytomedicine. 6 (1999) 119–123, https://doi.org/10.1016/S0944-7113(99)80046-4.

[32] B. Kandasubramanian, R. Yadav, F. Dixit, T.J. Sahetya, POLYMER MEMBRANE AND THE PROCESS OF PREPARING THE SAME, 601/MUM/2013, 2013.

[33] X. Xiong, P. Wang, K. Su, W.C. Cho, Y. Xing, Chinese herbal medicine for coronavirus disease 2019: A systematic review and meta-analysis, Pharmacol. Res. 160 (2020), 105056, https://doi.org/10.1016/j.phrs.2020.105056.

[34] R.A.C. Siemieniuk, J.J. Bartoszko, L. Ge, D. Zeraatkar, A. Izcovich, H. Pardo-Hernandez, B. Rochwerg, F. Lamontagne, M.A. Han, E. Kum, Q. Liu, A. Agarwal, T. Agoritsas, P. Alexander, D.K. Chu, R. Couban, A. Darzi, T. Devji, B. Fang, C. Fang, S.A. Flottorp, F. Foroutan, D. Heels-Ansdell, K. Honarmand, L. Hou, X. Hou, Q. Ibrahim, M. Loeb, M. Marcucci, S.L. McLeod, S. Motaghi, S. Murthy, R. A. Mustafa, J.D. Neary, A. Qasim, G. Rada, I. Bin Riaz, B. Sadeghirad, N. Sekercioglu, L. Sheng, C. Switzer, B. Tendal, L. Thabane, G. Tomlinson, T. Turner, P.O. Vandvik, R.W.M. Vernooij, A. Viteri-García, Y. Wang, L. Yao, Z. Ye, G.H. Guyatt, R. Brignardello-Petersen, Drug treatments for covid-19: Living systematic review and network meta-Analysis, BMJ. 370 (2020), m2980, https://doi.org/10.1136/bmj.m2980.

[35] I. Bartoňková, Z. Dvořák, Assessment of endocrine disruption potential of essential oils of culinary herbs and spices involving glucocorticoid, androgen and vitamin D receptors, Food Funct. 9 (2018) 2136–2144, https://doi.org/10.1039/c7fo02058a.

[36] M.F. Bashir, B. Ma, L. Shahzad, A brief review of socio-economic and environmental impact of Covid-19, Air Qual. Atmos. Heal. (2020), https://doi.org/10.1007/s11869-020-00894-8.

[37] M.A. Chowdhury, M.B.A. Shuvho, M.A. Shahid, A.K.M.M. Haque, M.A. Kashem, S.S. Lam, H.C. Ong, M.A. Uddin, M. Mofijur, Prospect of biobased antiviral face mask to limit the coronavirus outbreak, Environ. Res. 192 (2021) 110294, https://doi.org/10.1016/j.envres.2020.110294.

[38] A. Nicosia, W. Gieparda, J. Foksowicz-Flaczyk, J. Walentowska, D. Wesołek, B. Vazquez, F. Prodi, F. Belosi, Air filtration and antimicrobial capabilities of electrospun PLA/PHB containing ionic liquid, Sep. Purif. Technol. 154 (2015) 154–160, https://doi.org/10.1016/j.seppur.2015.09.037.

[39] Y. Tokiwa, B.P. Calabia, Biodegradability and biodegradation of poly(lactide), Appl. Microbiol. Biotechnol. 72 (2006) 244–251, https://doi.org/10.1007/s00253-006-0488-1.

[40] P.M. Gore, B. Kandasubramanian, Heterogeneous wettable cotton based superhydrophobic Janus biofabric engineered with PLA/functionalized-organoclay microfibers for efficient oil–water separation, J. Mater. Chem. A. 6 (2018) 7457–7479, https://doi.org/10.1039/C7TA11260B.

[41] P.M. Gore, M. Naebe, X. Wang, B. Kandasubramanian, Silk Fibres Exhibiting Biodegradability & Superhydrophobicity for Recovery of Petroleum Oils from Oily Wastewater, J. Hazard. Mater. (2019) 121823, https://doi.org/10.1016/j.jhazmat.2019.121823.

[42] P.M. Gore, M. Naebe, X. Wang, B. Kandasubramanian, Progress in silk materials for integrated water treatments: Fabrication, modification and applications, Chem. Eng. J. 374 (2019) 437–470, https://doi.org/10.1016/j.cej.2019.05.163.

[43] C. Zinge, B. Kandasubramanian, Nanocellulose based biodegradable polymers, Eur. Polym. J. 133 (2020), 109758, https://doi.org/10.1016/j.eurpolymj.2020.109758.

[44] D.G. Prajapati, B. Kandasubramanian, Biodegradable Polymeric Solid Framework-based Organic Phase Change Materials for Thermal Energy Storage, (2019). 10.1021/acs.iecr.9b01693.

[45] C.H. Park, Y.K. Kang, S.S. Im, Biodegradability of cellulose fabrics, J. Appl. Polym. Sci. 94 (2004) 248–253, https://doi.org/10.1002/app.20879.

[46] L. Li, M. Frey, K.J. Browning, Biodegradability study on cotton and polyester fabrics, J. Eng. Fiber. Fabr. 5 (2010) 42–53, https://doi.org/10.1177/155892501000500406.

[47] A.O. Ameh, M.T. Isa, E.K. Udoka, Biodegradable detergents from Azadirachta Indica (neem) seed oil, Leonardo Electron. J. Pract. Technol. 9 (2010) 69–74.

[48] P. Govindaraj, B. Kandasubramanian, K.M. Kodam, Molecular interactions and antimicrobial activity of curcumin (Curcuma longa) loaded polyacrylonitrile films, Mater. Chem. Phys. 147 (2014) 934–941, https://doi.org/10.1016/j.matchemphys.2014.06.040.

[49] R. Yadav, B. Kandasubramanian, Egg albumin PVA hybrid membranes for antibacterial application, Mater. Lett. 110 (2013) 130–133, https://doi.org/10.1016/j.matlet.2013.07.109.

[50] B. Kandasubramanian, P. Pillai, THE PROCESS FOR EXTRACTION OF ESSENTIAL OIL AND THE PRODUCT OBTAIN THEREFORE, 640/MUM/2014, 2014.

[51] B. Kandasubramanian, P. Pillai, ANTIMICROBIAL POLYMER MATRIX AND PROCESS FOR PREPARING THE SAME, 619/MUM/2014, 2014.

[52] Bureau of Indian Standards, Medical Textiles - Surgical Face Masks - Specification, IS 16289:2014, 2019.

[53] Bureau of Indian Standards, Medical Textiles — Method for Evaluation of the Bacterial Filtration Efficiency of Surgical Face Masks, IS 16288:2014, 2019.

[54] S. Jiang, H. Li, L. Piao, Z. Jin, J. Liu, S. Chen, L.L. Liu, Y. Shao, B. Zhong, B. Wu, W. Li, J. Ren, Y. Zhang, H. Wang, R. Jin, Computational study on new natural compound inhibitors of indoleamine 2,3-dioxygenase 1, Aging (Albany. NY). 12 (2020) 11349–11363. 10.18632/aging.103113.

[55] L. Jiang, X. Zhang, X. Chen, Y. He, L. Qiao, Y. Zhang, G. Li, Y. Xiang, Virtual screening and molecular dynamics study of potential negative allosteric modulators of mGluR1 from Chinese herbs, Molecules. 20 (2015) 12769–12786, https://doi.org/10.3390/molecules200712769.

[56] S.N. Rao, M.S. Head, A. Kulkarni, J.M. LaLonde, Validation studies of the site-directed docking program LibDock, J. Chem. Inf. Model. 47 (2007) 2159–2171, https://doi.org/10.1021/ci6004299.

[57] A. Fagerlin, T.S. Valley, A.M. Scherer, M. Knaus, E. Das, B.J. Zikmund-Fisher, Communicating infectious disease prevalence through graphics: Results from an

international survey, Vaccine. 35 (2017) 4041–4047, https://doi.org/10.1016/j.vaccine.2017.05.048.

[58] S. Skariyachan, A.S. Setlur, S.Y. Naik, Enhanced biodegradation of low and high-density polyethylene by novel bacterial consortia formulated from plastic-contaminated cow dung under thermophilic conditions, (2017). 10.1007/s11356-017-8537-0.

[59] H. Li, Z. Wang, H. Zhang, Z. Pan, Nanoporous PLA/(Chitosan Nanoparticle) composite fibrous membranes with excellent air filtration and antibacterial performance, Polymers (Basel) 10 (2018) 10–12, https://doi.org/10.3390/polym10101085.

[60] Q. Shi, C. Zhou, Y. Yue, W. Guo, Y. Wu, Q. Wu, Mechanical properties and in vitro degradation of electrospun bio-nanocomposite mats from PLA and cellulose nanocrystals, Carbohydr. Polym. 90 (2012) 301–308, https://doi.org/10.1016/j.carbpol.2012.05.042.

[61] X. Xu, X. Chen, X. Jing, Biodegradable electrospun poly (L -lactide) fibers containing antibacterial silver nanoparticles, Eur. Polym. J. 42 (2006) 2081–2087, https://doi.org/10.1016/j.eurpolymj.2006.03.032.

[62] W. Teo, R. Inai, S. Ramakrishna, Technological advances in electrospinning of nanofibers, Sci. Technol. Adv. Fibres. 013002 (2011), https://doi.org/10.1088/1468-6996/12/1/013002.

[63] F. Zhou, R. Gong, I. Porat, Mass production of nanofibre assemblies by electrostatic spinning, Polym. Int. (2009) 331–342, https://doi.org/10.1002/pi.2521.

[64] P. Kozlik, Z. Bosakova, D. Marekova, V. Holan, E. Sykova, Controlled gentamicin release from multi-layered electrospun nanofibrous structures of various thicknesses, Int. J. Nanomedicine. 5315–5325 (2012).

[65] Z. Wang, Z. Pan, Preparation of hierarchical structured nano-sized/porous poly (lactic acid) composite fibrous membranes for air filtration, Appl. Surf. Sci. 356 (2015) 1168–1179, https://doi.org/10.1016/j.apsusc.2015.08.211.

[66] M.K. Selatile, S.S. Ray, V. Ojijo, R. Sadiku, Depth filtration of airborne agglomerates using electrospun bio-based polylactide membranes, J. Environ. Chem. Eng. 6 (2018) 762–772, https://doi.org/10.1016/j.jece.2017.12.070.

[67] X. Chen, Y. Xu, M. Liang, Q. Ke, Y. Fang, H. Xu, X. Jin, C. Huang, Honeycomb-like polysulphone/polyurethane nanofiber filter for the removal of organic/inorganic species from air streams, J. Hazard. Mater. (2018), https://doi.org/10.1016/j.jhazmat.2018.01.012.

[68] S. Yan, The formation of ultrafine polyamide 6 nanofiber membranes with needleless electrospinning for air filtration, Polym. Adv. Technol. (2019) 1–9, https://doi.org/10.1002/pat.4594.

[69] L. Wang, C. Zhang, G. Pan, Needleless electrospinning for scaled-up production of ultrafine chitosan hybrid nanofibers used for air filtration, RSC Adv. (2016), https://doi.org/10.1039/C6RA24557A.

[70] A.K. Selvam, G. Nallathambi, Polyacrylonitrile/silver nanoparticle electrospun nanocomposite matrix for bacterial filtration, Fibers Polym. 16 (2015) 1327–1335, https://doi.org/10.1007/s12221-015-1327-8.

[71] S. Zhang, H. Liu, X. Yin, Z. Li, J. Yu, B. Ding, Tailoring mechanically robust poly (m-phenylene isophthalamide) nanofiber/nets for ultrathin high-efficiency air filter, Sci. Rep. 7 (2017) 1–11, https://doi.org/10.1038/srep40550.

[72] X. Qin, S. Wang, Filtration properties of electrospinning nanofibers, J. Appl. Polym. Sci. (2006), https://doi.org/10.1002/app.24361.

[73] M. Zhu, J. Han, F. Wang, W. Shao, R. Xiong, Q. Zhang, H. Pan, Y. Yang, S. K. Samal, F. Zhang, C. Huang, Electrospun Nanofibers Membranes for Effective Air Filtration, Macromol. Mater. Eng. 302 (2017) 1–27, https://doi.org/10.1002/mame.201600353.

[74] C.D. Zangmeister, J.G. Radney, E.P. Vicenzi, J.L. Weaver, Filtration Efficiencies of Nanoscale Aerosol by Cloth Mask Materials Used to Slow the Spread of SARS CoV-2, (2020). https://doi.org/10.1021/acsnano.0c05025.

[75] M. Hajikhani, Z. Emam-Djomeh, G. Askari, Fabrication and characterization of mucoadhesive bioplastic patch via coaxial polylactic acid (PLA) based electrospun nanofibers with antimicrobial and wound healing application, Int. J. Biol. Macromol. 172 (2021) 143–153, https://doi.org/10.1016/j.ijbiomac.2021.01.051.

[76] P.M. Gore, M. Dhanshetty, Bionic creation of nano-engineered Janus fabric for selective oil/organic solvent absorption, RSC Adv. 6 (2016) 111250–111260, https://doi.org/10.1039/C6RA24106A.

[77] P.M. Gore, A. Purushothaman, M. Naebe, X. Wang, B. Kandasubramanian, Nanotechnology for Oil-Water Separation, in: R. Prasad, T. Karchiyappan (Eds.), Adv. Res. Nanosci. Water Technol., 1st ed., Springer Nature Switzerland AG, Cham, 2019: pp. 299–339. https://doi.org/10.1007/978-3-030-02381-2_14.

[78] R. Zyschka, FACE MASKS, Tübingen, 2020. https://www.cht.com/cht/medien.nsf/gfx/med_MJOS-BN9GJM_4395D1/$file/CHT-Group-textile-face-masks.pdf.

[79] O. Gavrilenko, X. Wang, Functionalized nanofibrous coating on cotton fabrics, Cellulose. 26 (2019) 4175–4190, https://doi.org/10.1007/s10570-019-02342-y.

[80] D. De Smet, D. Weydts, M. Vanneste, Environmentally friendly fabric finishes, in: R. Blackburn (Ed.), Sustain. Appar. Prod. Process. Recycl., 1st ed., Elsevier, New York, 2015: pp. 3–33. https://doi.org/10.1016/B978-1-78242-339-3.00001-7.

[81] I. Rezić, A. Kiš, Design of Experiment Approach to Optimize Hydrophobic Fabric Treatments, Polymers (Basel). 12 (2020) 2131, https://doi.org/10.3390/polym12092131.

[82] N. Deoray, B. Kandasubramanian, Review on Three-Dimensionally Emulated Fiber-Embedded Lactic Acid Polymer Composites: Opportunities in Engineering Sector, Polym. - Plast. Technol. Eng. 57 (2018) 860–874, https://doi.org/10.1080/03602559.2017.1354226.

[83] P. Gupta, B. Kandasubramanian, Directional Fluid Gating by Janus Membranes with Heterogeneous Wetting Properties for Selective Oil-Water Separation, ACS Appl. Mater. Interfaces. 9 (2017) 19102–19113, https://doi.org/10.1021/acsami.7b03313.

[84] A.B.D. Cassie, S. Baxter, Wettability of porous surfaces, Trans. Faraday Soc. 40 (1944) 546–551, https://doi.org/10.1039/tf9444000546.

[85] A.E. Purushothaman, K. Thakur, B. Kandasubramanian, Development of highly porous, Electrostatic force assisted nanofiber fabrication for biological applications, Int. J. Polym. Mater. Polym. Biomater. (2019) 1–28, https://doi.org/10.1080/00914037.2019.1581197.

[86] K. Thakur, A. Rajhans, B. Kandasubramanian, Starch/PVA hydrogels for oil/water separation, Environ. Sci. Pollut. Res. (2019), https://doi.org/10.1007/s11356-019-06327-z.

[87] J. Choi, B.J. Yang, G.N. Bae, J.H. Jung, Herbal Extract Incorporated Nanofiber Fabricated by an Electrospinning Technique and its Application to Antimicrobial Air Filtration, ACS Appl. Mater. Interfaces. 7 (2015) 25313–25320, https://doi.org/10.1021/acsami.5b07441.

[88] A. Ali, M.A. Shahid, M.D. Hossain, M.N. Islam, Antibacterial bi-layered polyvinyl alcohol (PVA)-chitosan blend nanofibrous mat loaded with Azadirachta indica (neem) extract, Int. J. Biol. Macromol. 138 (2019) 13–20, https://doi.org/10.1016/j.ijbiomac.2019.07.015.

[89] M. Koena Selatile, V. Ojijo, R. Sadiku, S. Sinha, Development of bacterial-resistant electrospun polylactide membrane for air filtration application : Effects of reduction methods and their loadings, Polym. Degrad. Stab. 178 (2020), 109205, https://doi.org/10.1016/j.polymdegradstab.2020.109205.

[90] A. Astani, J. Reichling, P. Schnitzler, Comparative Study on the Antiviral Activity of Selected Monoterpenes Derived from Essential Oils, 679 (2010) 673–679. https://doi.org/10.1002/ptr.2955.

[91] M.D. Antunes, G. da Silva Dannenberg, M. Fiorentini, Z. Pinto, L.-T. Lim, E. da R. Zavareze, A.R.G. Dias, Antimicrobial electrospun ultrafine fibers from zein containing eucalyptus essential oil/cyclodextrin inclusion complex, Int. J. Biol. Macromol. (2017), https://doi.org/10.1016/j.ijbiomac.2017.06.095.

[92] S.A. Kulkarni, S.K. Nagarajan, V. Ramesh, V. Palaniyandi, S.P. Selvam, T. Madhavan, Computational evaluation of major components from plant essential oils as potent inhibitors of SARS-CoV-2 spike protein, J. Mol. Struct. 1221 (2020), 128823, https://doi.org/10.1016/j.molstruc.2020.128823.

[93] V. Schnecke, C.A. Swanson, E.D. Getzoff, J.A. Trainer, L.A. Kuhn, Screening a peptidyl database for potential ligands to proteins with side-chain flexibility, Proteins Struct. Funct. Genet. 33 (1998) 74–87, https://doi.org/10.1002/(SICI)1097-0134(19981001)33:1<74::AID-PROT7>3.0.CO;2-L.

[94] L. Zhou, J. Wang, K. Wang, J. Xu, J. Zhao, T. Shan, C. Luo, Secondary metabolites with antinematodal activity from higher plants, Elsevier (2012), https://doi.org/10.1016/B978-0-444-59514-0.00003-1.

[95] K. Bhatt, D.K. Maheshwari, Decoding multifarious role of cow dung bacteria in mobilization of zinc fractions along with growth promotion of C. annuum L, Sci. Rep. (2019) 1–10, https://doi.org/10.1038/s41598-019-50788-8.

[96] O. Obire, S.B. Akinde, Aerobic heterotrophic bacteria and petroleum-utilizing bacteria from cow dung and poultry manure, World J. Microbiol. Biotechnol. (2008) 1999–2002, https://doi.org/10.1007/s11274-008-9700-z.

[97] S.A. Adebusoye, O.O. Amund, O.D. Teniola, S.O. Olatope, Microbial degradation of petroleum hydrocarbons in a polluted tropical stream, World J. Microbiol. Biotechnol. (2007) 1149–1159, https://doi.org/10.1007/s11274-007-9345-3.

[98] N. Kumar, M. Kumar, C. Mudenur, A. Kalamdhad, Biodegradation of modi fied Poly (lactic acid) based biocomposite films under thermophilic composting conditions, Polym. Test. 76 (2019) 522–536, https://doi.org/10.1016/j.polymertesting.2019.02.021.

[99] M. Agarwal, K.W. Koelling, J.J. Chalmers, Characterization of the Degradation of Polylactic Acid Polymer in a Solid Substrate Environment, Biotechnol. Prog. (1998) 517–526, https://doi.org/10.1021/bp980015p.

[100] T. Yamada, H. Tsuji, H. Daimon, H. Tsuji, H. Daimon, Improvement of methanogenic activity of anaerobic digestion using poly(lactic L-acid) with enhanced chemical hydrolyzability based on physicochemical parameters, J. Environ. Manage. (2018), https://doi.org/10.1016/j.jenvman.2018.08.034.

[101] S. Machado, A. Ferraz, Biological pretreatment of sugarcane bagasse with basidiomycetes producing varied patterns of biodegradation, Bioresour. Technol. (2016), https://doi.org/10.1016/j.biortech.2016.11.053.

[102] A.G. Costa, G.C. Pinheiro, F.G.C. Pinheiro, A.B. Dos Santos, S.T. Santaella, R. C. Leitão, The use of thermochemical pretreatments to improve the anaerobic biodegradability and biochemical methane potential of the sugarcane bagasse, Chem. Eng. J. 248 (2014) 363–372, https://doi.org/10.1016/j.cej.2014.03.060.